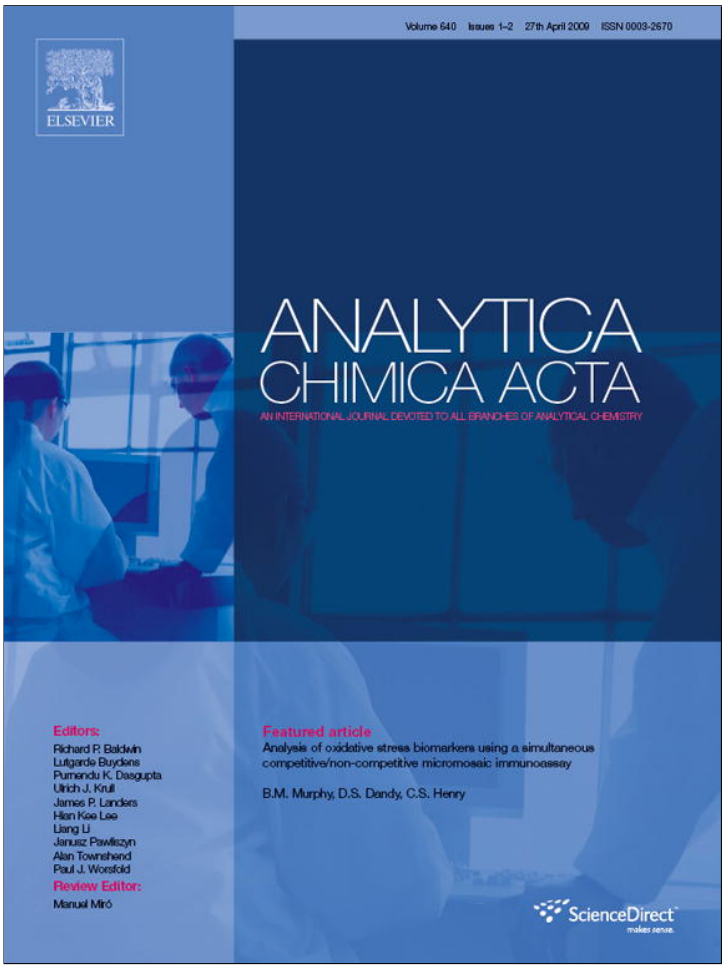

Analytica Chimica Acta 640 (2009) 1–6

Contents lists available at ScienceDirect

Analytica Chimica Acta

journal homepage: www.elsevier.com/locate/aca

Analysis of oxidative stress biomarkers using a simultaneous competitive/non-competitive micromosaic immunoassay

Brian M. Murphy[a], David S. Dandy[b], Charles S. Henry[a,b,*]

[a] Department of Chemistry, Colorado State University, Fort Collins, CO 80523, USA
[b] Department of Chemical and Biological Engineering, Colorado State University, Fort Collins, CO 80523, USA

ARTICLE INFO

Article history:
Received 19 November 2008
Received in revised form 23 February 2009
Accepted 2 March 2009
Available online 17 March 2009

Keywords:
Immunoassay
Micromosaic
Microfluidics
Multi-analyte analysis
High throughput
Immunoaffinity array

ABSTRACT

Immunoassays represent a core workhorse methodology for many applications ranging from clinical diagnostics to environmental monitoring. In traditional formats such as the enzyme linked immunosorbent assay (ELISA), analytes are measured singly or in small sets. As more biomarkers are identified for disease states, there is a need to develop methods that can measure multiple markers simultaneously. Immunoaffinity arrays are one such chemistry that can achieve multi-marker screening. Most arrays are performed in either competitive or non-competitive formats, where the former are used predominantly for small molecules and the later for macromolecules. To date, ELISA and immunoaffinity array methods have relied exclusively on one of these formats and not the other. Here an immunoaffinity array method capable of performing simultaneous competitive and non-competitive analysis generated using micromosaic immunoassay techniques is introduced for the analysis of metabolites and proteins. In this report, three markers of oxidative stress were used as a model system. The method described here demonstrates the simultaneous analysis of 3-nitrotyrosine, by indirect competitive immunoassay while the enzymes catalase and superoxide dismutase are analyzed by non-competitive sandwich immunoassay. The method requires less than 1 μL sample and 45 min for completion. Logistic curve fits and LOD (limits of detection) statistical analysis of the binding results are presented and show good agreement with published data for these antibody–antigen systems.

1. Introduction

Rapid, reliable identification of trace markers from complex biological samples (serum, food, environment, etc.) at μg–pg mL^{-1} levels is essential in food safety, medicine, environmental chemistry, fundamental biochemistry and molecular biology and biosecurity. Direct detection of trace markers from complex samples is often over-whelmed by high concentration, confounding, non-analyte proteins and metabolites. Bioanalytical selectivity and sensitivity to this increasing list of targets requires improved analytical methods. Immunoassays represent a reliable, well-known approach to address this problem and thus represent an important core workhorse technology [1]. They are among the most specific of analytical techniques, provide low detection limits (on the order of pg mL^{-1}), and can be used for a wide range of substances [2]. Immunoassays demonstrate both high selectivity due to antigen/antibody interactions and high sensitivity due to fluorescent, chemiluminescent, or radioactive labels [3]. Traditional immunoassays are, however, labor and time intensive due to multiple wash and incubation steps, and can only detect a *few* proteins or metabolites from any one sample in a single experiment. As a result, new methods based on arrays of selective binding agents, so-called immunoaffinity arrays, have been developed to increase throughput [4].

Immunoaffinity arrays represent an important step forward in high-throughput, multi-analyte screening of complex samples. In their highest density formats, hundreds to thousands of antibodies are deposited on a surface using one of a variety of special methods for spotting [5]. These arrays require specialized spotting instruments and array surfaces to ensure consistency of spot size and integrity. Low density arrays can be generated using a variety of simplified spotting methods on a wide range of surfaces. For example, Gale's laboratory has developed a continuous flow microfluidic device that can deposit proteins on a surface in a simple and reproducible manner [6–9]. Other methods have used spotting as well and have been reviewed extensively [10]. The Delamarche and Ligler groups pioneered the development of micromosaic immunoassays [11–18]. In micromosaic immunoassays, the surface is patterned using microfluidic channels to deliver solutions to defined locations on the surface. After patterning in the initial direction with one set of channels, a second set of channels is placed on the same surface in a perpendicular

* Corresponding author. Tel.: +1 970 491 1801; fax: +1 970 491 2852.
E-mail address: cshenry@lamar.colostate.edu (C.S. Henry).

0003-2670/$ – see front matter © 2009 Elsevier B.V. All rights reserved.
doi:10.1016/j.aca.2009.03.003

orientation to deliver sample. The resulting arrays are a series of squares that align themselves in a mosaic pattern, giving the technique its name. Initial work in this field (and the majority of immunoaffinity arrays) used non-competitive methods for detection of macromolecules. Our group recently reported the use of micromosaic assays for competitive analysis to allow for detection of metabolites [19]. What is lacking in this arena is the development of methods that can simultaneously measure both metabolites and proteins using simultaneous competitive and non-competitive immunoassays on the same surface. In this report, the development of a simultaneous competitive/non-competitive immunoassay for the detection of metabolites and proteins is presented. For a model system we detect three markers of oxidative stress.

The presence of molecular oxygen in the atmosphere presents a double-edged sword for humans and other species. The superoxide anion, O^{2-}, and other reactive oxygen species (ROS) are essential for cellular signaling [20] and the antimicrobial action of phagocytes [21], but are harmful at higher levels. ROS have been observed to cause oxidative damage to proteins [22], DNA [23], lipids [24], and other biomolecules, and have also been associated with numerous diseases including cancer [2], diabetes [25], atherosclerosis [26], and play a role in aging [27]. When the anti-oxidant system is overcome by oxidative processes, the organism is said to be under oxidative stress during which oxidative damage can occur [28]. Antioxidants and products of oxidative stress have received much attention due to the implication of oxidative damage in disease. As analytical targets, these species can be used to assess antioxidant capacity or oxidative status in vitro [29]. However, due to the complexity of the antioxidant system and because a universal marker for oxidative stress has not been identified, analysis of multiple markers is preferred when assessing oxidative status [30–33]. Therefore, there is a need for bioanalytical methods capable of parallel, high-throughput analysis of oxidative stress biomarkers.

An analysis of three oxidative stress biomarkers using a micromosaic immunoassay is presented [16]. The micromosaic format has been previously demonstrated for the analysis of cardiac biomarkers (sandwich immunoassay) [34], cell surface receptors [12], and most recently the thyroid hormone thyroxine (competitive immunoassay) [19]. However, no micromosaic method has been developed for concerted analysis of both metabolites and macromolecules. This development is important because it will provide the ability to simultaneously measure both small and large molecules from a single sample. Here, the small molecule 3-nitrotyrosine (3NT) is examined by indirect competitive immunoassay, while bovine enzyme antioxidants catalase (CAT) and superoxide dismutase (Cu,Zn SOD/SOD1) are analyzed by sandwich (non-competitive) immunoassay. Each of the analytes has been proposed as a marker of oxidative status. By adding a third patterning step to the micromosaic assay, it is demonstrated for the first time that competitive and sandwich immunoassays can be performed in parallel using the micromosaic method. This work demonstrates that micromosaic immunoassays can function as a rapid, high throughput method for simultaneous competitive and non-competitive analysis of biomarkers.

2. Methods

2.1. Chemicals and materials

Unless otherwise noted, all chemicals were purchased from Sigma (St. Louis, MO). Anti-bovine SOD (Cu, Zn) (rabbit pAb IgG, S8060-11), anti-bovine catalase (rabbit pAb IgG, C2096-06), and anti-3-nitrotyrosine (mouse mAb IgG1, N2700-09) were purchased from United States Biological (Swampscott, MA). Catalase from bovine liver (C9322), bovine superoxide dismutase (S7571), and 3-nitro-L-tyrosine (N7389) were purchased from Sigma. Fluorescent measurements were made using a Photometrics HQ2 CCD camera from Roper Scientific (Tuscon, AZ) and MetaMorph 7.1.7 software from Molecular Devices (Sunnyvale, CA) using a Nikon Eclipse TE2000-U epifluorescence microscope (Melville, NY). Poly (dimethylsiloxane) (PDMS, Sylgard 184) was obtained from Dow Corning (Midland, MI) and used at a 10:1 ratio of monomer to crosslinker. SU8-2035 photoresist was purchased from Microchem (Newton, MA). AlexaFluor® 488 Monoclonal Antibody Labeling Kit (A20181) was purchased from Invitrogen (Carlsbad, CA). Slide-A-Lyzer MINI Dialysis Units were purchased from Pierce (Rockford, IL). Silicon nitride wafers with a proprietary coating were received as a gift from Biostar (Boulder, CO). [35] 1.5 mm biopsy punches were obtained from Robbins Instruments (Chatham, NJ). All chemicals were used as received.

2.2. Protein labeling and conjugation

Prior to use, all antibodies were purified by dialysis for 2 h against 1L of 25 mM phosphate, 150 mM NaCl pH 7.4 (PBS). Capture antibodies (pAb SOD, pAb CAT) were diluted to the specified concentrations using deionized water. Detection antibodies for both competitive (mAb 3NT) and sandwich assays (pAb SOD, pAb CAT) were prepared at 1 mg mL^{-1} in 100 μL of the above mentioned buffer and labeled with AlexaFluor® 488 (AF) using the AlexaFluor® 488 Monoclonal Antibody Labeling Kit. Labeled antibodies were purified according to the directions included with the kit and were stored at 4 °C until use. 3NT was conjugated to bovine serum albumin (BSA) using carbodiimide chemistry as described in the literature. [36] The hapten was solublized for conjugation in a 1:1 mixture of dimethylsulfoxide and 50 mM sodium phosphate, pH 8.5. The BSA-3NT conjugate was dialyzed against PBS to remove unreacted hapten and EDC carbodiimide, stored at 0 °C prior to use in immunoassays and diluted with deionized water (Millipore, 18 Ω) to the final concentration prior to use.

2.3. Microfluidic network fabrication and substrate preparation

Microfluidic networks (μFNs) made from the polymer poly-(dimethylsiloxane) (PDMS) were used to pattern capture reagents and deliver analytes and affinity probes to the substrate. Negative relief molds for each network of channels were made using photolithography according to the literature [37,38]. Photolithography masks were designed in Adobe Illustrator and printed at 40,640 DPI by Fineline Imaging, Inc (Colorado Springs, CO). First and second dimension channels were designed with a 40 μm width and 20 μm spacing between channels. Actual channel dimensions were found to be 25 μm with a spacing of 35 μm and a height of 20 μm using profilometry. Third dimension μFNs were designed with single entry and exit ports and a 1.5 mm channel containing a central 3.0 mm diameter "bubble cell" design for patterning over the entire affinity mosaic. PDMS networks made using these molds were punched with a 1.5 mm biopsy punch to create wells for sample introduction. T-poly coated silicon nitride wafers (SiNx) were rinsed in Millipore water and dried under a stream of nitrogen prior to use. Wafers were scored and cut into pieces approximately 1.5 cm × 1.5 cm for each assay.

2.4. Micromosaic immunoassays

All assays were performed using three patterning steps or "dimensions." μFNs were made hydrophilic before each patterning

step by oxidation in an air plasma cleaner for 50 s at 18 W. A volume of 0.9 μL of reagent was introduced to each well at each step. First dimension patterning was used to sensitize the substrate with patterns of receptor proteins. The BSA conjugate of 3NT (BSA-3NT, 0.35 mg mL^{-1}) along with pAb SOD (0.66 mg mL^{-1}) and pAb CAT (0.30 mg mL^{-1}) in deionized water were patterned in triplicate for a 10 min incubation. Because the sensitizing agents were passively adsorbed, random orientation of the protein on the substrate was expected. μFNs were removed under PBS containing 0.05% Tween 20 (PBS-T), then rinsed copiously with PBS-T and water. Remaining reactive adsorption sites were passivated by a 5 min incubation with 0.5 mL 45 mg mL^{-1} BSA in PBS covering the entire substrate. This was followed by repeating the above rinse procedure. Solutions containing all three analytes and competitive assay tracer AF mAb 3NT (25 μg mL^{-1}) in 45 mg mL^{-1} human serum albumin (HSA) were patterned orthogonal to the first dimension pattern for 15 min and rinsed. A schematic of the steps required for immunoassay is described in the literature, and the steps required for sandwich immunoassay are depicted in Fig. 1 [19]. Finally, detection reagents for the two sandwich assays (AF pAb SOD, 50 μg mL^{-1} and AF pAb CAT, 50 μg mL^{-1}) in 45 mg mL^{-1} BSA/PBS were patterned for 2.5 min using the "bubble cell" μFN that covered the entire mosaic area. Epifluorescence measurement parameters were a 4 × 4 binning, 10× objective, unmodified gain, and an exposure time of 1.5 s. Fluorescence measurements were taken directly from the image; no image processing or smoothing was applied. The average signal from each mosaic was recorded. Total assay time from the first patterning step to the fluorescence measurement was less than 45 min.

3. Results

3.1. Cross reactivity analysis

Prior to quantification of analyte in the multi-analyte immunoassay, a patterning experiment was carried out to determine possible cross-reactivity between tracer/detection antibodies and surface receptors/captured antigens. This was particularly important given the nature of the simultaneous competitive/non-competitive assays to be done in these experiments. Since no other reports have used this approach, we felt it important to consider this question in detail. Following sensitization, the competitive assay tracer (25 μg mL^{-1} AF pAb 3NT) and each antigen (10 ng mL^{-1} SOD, 125 ng mL^{-1} CAT) were patterned independently in triplicate, and the third dimension pattern followed this step as described above. A fluorescent image of this mosaic is shown in Fig. 2. Cross reactivity may be assessed by examining the fluorescent signal across each row. For example, signal from the middle three rows, in which AF mAb 3NT was patterned, shows that binding of the tracer to affinity mismatch coordinates (immobilized pAb CAT, pAb SOD) is below the sensitivity of the camera. In the bottom set of rows, pAb CAT captures only CAT, while the pAb CAT columns show only pAb CAT captures CAT. Specificity of detection antibodies for SOD and CAT were verified in a similar experiment utilizing only one detection antibody in the third patterning step in the presence of both captured targets. The results of this experiment show low cross reactivity for the prescribed antibodies and antigens, and therefore demonstrate that these three analytes can be measured simultaneously in the micromosaic format. This is an important finding

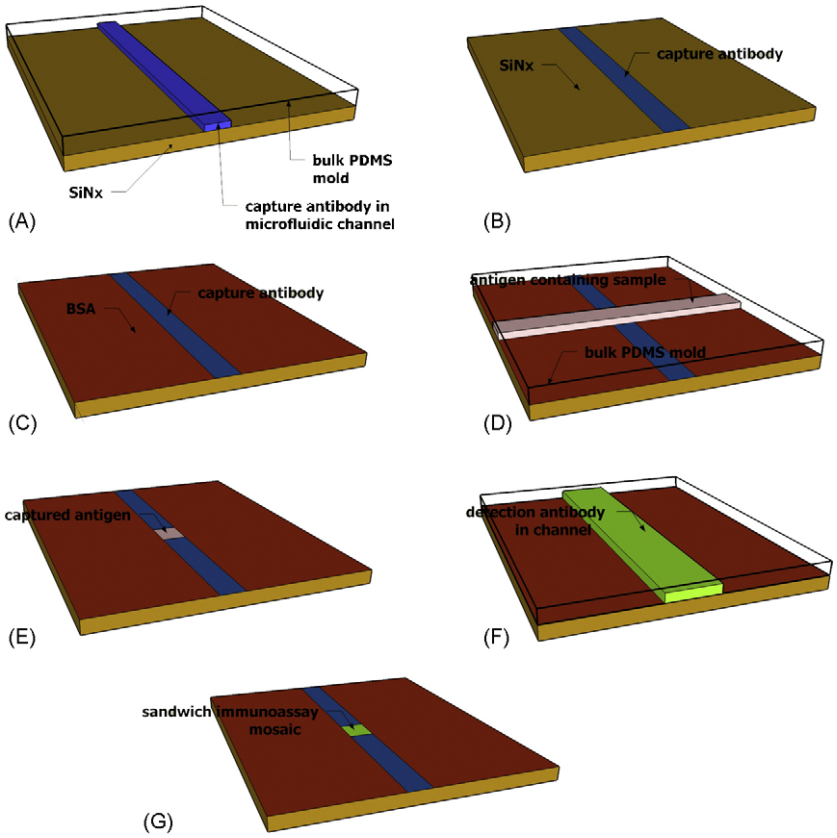

Fig. 1. Schematic of surface patterning for a sandwich immunoassay. (A) Substrate is sensitized with the appropriate capture antibody. (B) PDMS channels is removed, leaving the patterned substrate. (C) Unpatterned sites on the substrate are blocked from non-specific binding with BSA. (D) Antigen containing sample is patterned perpendicular to the first dimension pattern. (E) PDMS is removed, leaving captured antigen. (F) Fluorescently labeled detection antibody is patterned over all captured antigens. (G) PDMS is removed, and fluorescence image of the substrate is acquired.

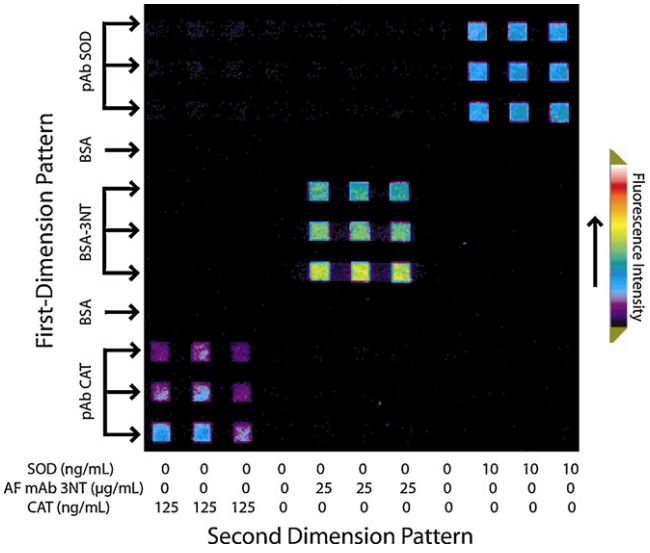

Fig. 2. Micromosaic demonstrating tracer specificity for patterned and captured proteins for each of the three analytical targets CAT, 3NT and SOD.

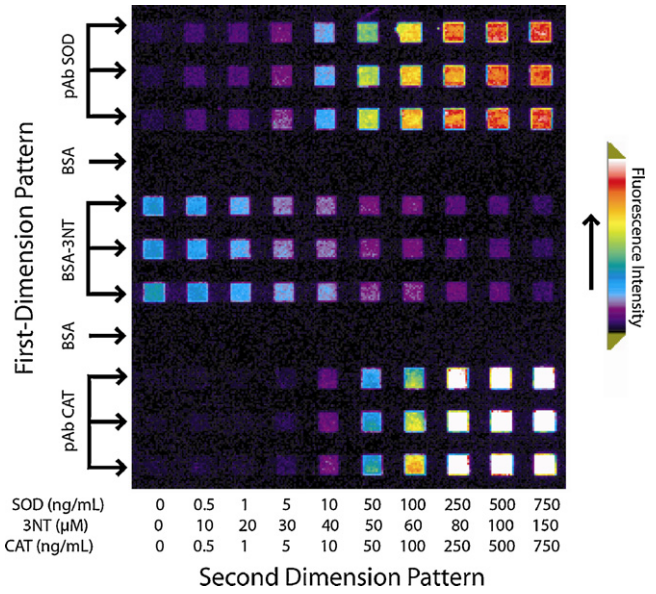

Fig. 3. Micromosaic immunoassay for simultaneous detection of CAT, 3NT, and SOD. Solutions patterned in the first and second dimension are indicated. The entire mosaic was patterned in the third dimension with 50 µg mL^{-1} AF pAb CAT and 50 µg mL^{-1} AF pAb SOD detection antibodies.

because it shows the ability to go forward with the simultaneous assay using the multistep patterning and labeling process.

3.2. Multiplexed immunoassay for CAT, 3NT, and SOD

After considering the cross-reactivity of the array, demonstration of the assay for all three analytes in a single sample was performed. Dilutions of CAT, 3NT, and SOD were prepared in 45 mg mL^{-1} HSA dissolved in phosphate buffered saline. While this is not a biological sample, it does represent a complex system containing physiologically relevant levels of albumin as thus serves as a good model system during experimental development. Prior to the multiplexed assay, each analyte was assayed individually to determine a working concentration range estimate. The appropriate titer of AF mAb 3NT was also determined experimentally [19]. These values were used to create dilutions containing the appropriate amount of each analyte. The fluorescent image of the three-analyte assay is shown in Fig. 3 with the corresponding concentrations of each analyte used in the second dimension pattern listed below. In the case of 3NT, the competitive effect is observed as signal decreases with increasing analyte concentration. In the cases of SOD and CAT, signal increases with increasing analyte concentration as expected until capture antibodies are saturated.

Dose-response curves for each assay were fit to the four-parameter logistic equation:

$$Y = \frac{a-d}{1+(T/c)^b} + d \quad (1)$$

where Y is the fluorescent signal (F/F_{max} where F_{max} is the highest signal observed for each analyte set), a is the response in absence of analyte, d is the response due to non-specific adsorption of tracer, c is the concentration of analyte that produces a signal $Y=(a+d)/2$, T is the analyte concentration, and b is the absolute value of the slope of the curve in a log–logit format [39]. Curves were fit using OriginPro 7's non-linear curve fitting tool for a four-parameter logistic equation using 300 iterations. Correlation coefficients were 0.999, 0.996, and 0.999 and reduced χ^2 values were 1×10^{-4}, 2×10^{-5}, and 4×10^{-5} for CAT, 3NT and SOD, respectively.

Dose-response curves are shown in Fig. 4. Error bars represent a single standard deviation for each set of three mosaic squares that correspond to one concentration of analyte. Error may be partially attributed to depletion of captured reagent (target protein or competitive assay tracer) during flow across the substrate. This phenomenon has been documented previously during a micromosaic immunoassay for C-Reactive protein [40]. The direction of flow in Fig. 3 was from the bottom of the image to the top. The depletion effect is most pronounced for CAT although it also contributes to the variability for 3NT. A fluorescence intensity profile linescan for the 100 ng mL^{-1} CAT mosaic in Fig. 3 is shown in Fig. 5 along with an indication of the direction of flow. This figure shows that depletion of CAT occurs not only between mosaics, but within them as well. SOD is least affected by error, having the lowest absolute signal deviation of all three analytes. These results suggest that depletion in micromosaic immunoassays are an analyte-dependent phenomenon. SOD (32 kDa) is much smaller than both rabbit IgG (150 kDa) and CAT (250 kDa), and will have a higher Stokes-Einstein diffusion coefficient, making the SOD assay less susceptible to depletion effects inherent to the mass transfer-limited conditions

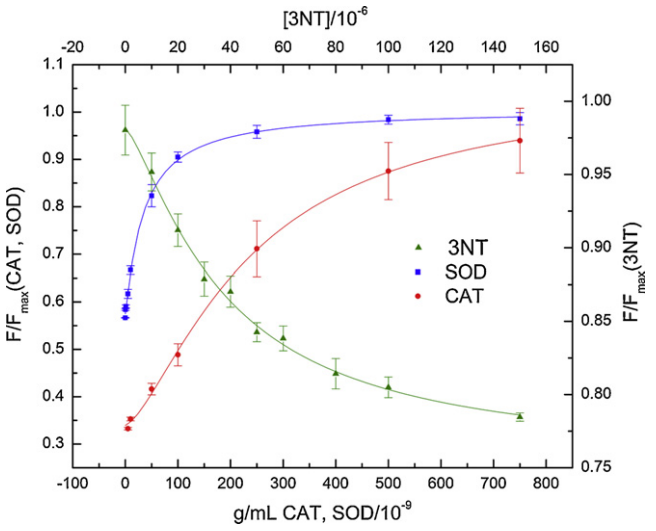

Fig. 4. Dose-response curves for CAT, 3NT, and SOD obtained from fluorescent signals in Fig. 3.

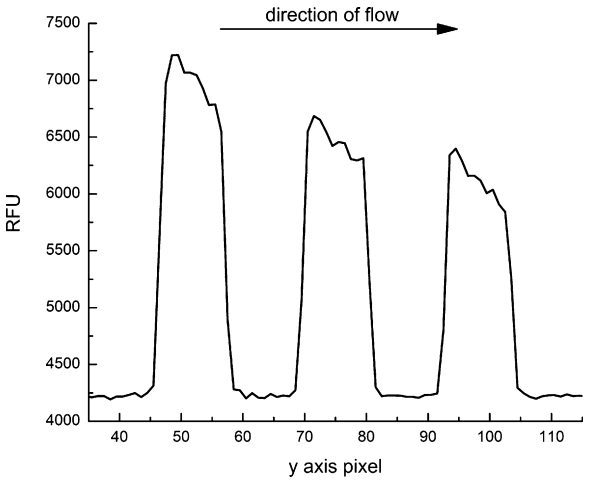

Fig. 5. Fluorescence intensity profile of 100 ng mL^{-1} CAT mosaics with direction of flow indicated. Depletion of analyte from solution occurs along the direction of flow.

in these experiments. Possible solutions to the depletion effect include analyzing a sample in three channels during second dimension patterning as opposed to using three sensitized channels in the first step, or increasing the spacing between channels during the sensitizing step.

3.3. Calculation of limits of detection

The LOD (limits of detection) for an immunoassay is given as the lowest concentration of analyte or dose which gives a signal statistically different from that at zero analyte concentration [36,41]. Å method for calculating detection limit estimates based on the standard deviation of mean response at zero-dose has been developed [42]. The expected response at the detection limit (Y_{min}) can be expressed as:

$$Y_{min} = Y_0 \pm ts\left[\frac{1}{n_0} + \frac{1}{n_{min}}\right]^{1/2} \quad (2)$$

where Y_0 is the mean response at zero dose, t is student's t at 95% CI, s is the standard deviation of the response near zero dose, and n_0 and n_{min} are the number of replicates performed at zero dose and at the theoretical LOD. In the case of a negative slope near zero dose (as in a competitive assay), the (+) is used in Eq. 2. In the case of a positive slope near zero dose (a two-site or sandwich assay), the (−) is used instead. Y_{min} can be substituted into the dose-response curve to obtain the calculated detection limit. In this work, s is taken as the average standard deviation from all data points assayed, except for the case of CAT where high-dose standard deviations were much larger than those found closer to zero dose; only the deviations from the lowest four responses were averaged. CAT also differs in that the signal at zero dose was below the camera sensitivity, so $Y = 5$ ng mL^{-1} was used in place of Y_0. After determining the response at the minimum detectable dose and substituting into the logistic curve fits (including error to those curve fits), the detection limits at 95% CI were found to be 35 ± 4.8 ng mL^{-1} CAT, 8 ± 1.4 μM 3NT, and 1.7 ± 0.14 ng mL^{-1} SOD. These detection limits are in the range of what is normal for immunoaffinity array techniques given the large variability in antibody properties.

3.4. Conclusions

Bernard et al. has demonstrated the use of micromosaics for detection of antigens using non-competitive sandwich immunoassay, while our lab has developed methodology for micromosaic competitive immunoassays [16,19]. In this work, the merging of the two micromosaic techniques is examined for the combined simultaneous competitive and sandwich immunoassay of a small molecule metabolite and two enzyme biomarkers for oxidative stress. The micromosaic method is shown to detect each analyte with low cross reactivity in a HSA/PBS matrix containing the other two analytes. Detection limits for catalase and superoxide dismutase were 35 ± 4.8 ng mL^{-1} and 1.7 ± 0.14 ng mL^{-1}, while for 3-nitrotyrosine the detection limit was 8 ± 1.4 μM. The immunoassay required less than 1 μL of sample, needed minimal user optimization, and could be completed within 45 min.

Acknowledgments

We thank the Dandy research group for their crucial advice and support and Scott Lynn for his help with photolithography mask design. This work was supported by National Institutes of Health grant EB00726.

References

[1] C.A. Marquette, L.J. Blum, Biosens. Bioelectron. 21 (2006) 1424.
[2] T.M. Hagen, S. Huang, J. Curnutte, P. Fowler, V. Martinez, C.M. Wehr, B.N. Ames, F.V. Chisari, Proc. Natl. Acad. Sci. U.S.A. 91 (1994) 12808.
[3] N.M. Schultz, L. Tao, D.J. Rose, R.T. Kennedy, in: J.P. Landers (Ed.), Handbook of Capillary Electrophoresis, CRC Press, Boca Raton, 1997, p. 611.
[4] U.B. Nielsen, B.H. Geierstanger, J. Immunol. Methods 290 (2004) 107.
[5] G. MacBeath, S.L. Schreiber, Science 289 (2000) 1760.
[6] S. Natarajan, A. Hatch, D.G. Myszka, B.K. Gale, Anal. Chem. 80 (2008) 8561.
[7] K.A. Smith, B.K. Gale, J.C. Conboy, Anal. Chem. 80 (2008) 7980.
[8] M.A. Eddings, A.R. Miles, J.W. Eckman, J. Kim, R.L. Rich, B.K. Gale, D.G. Myszka, Anal. Biochem. 382 (2008) 55.
[9] S. Natarajan, P.S. Katsamba, A. Miles, J. Eckman, G.A. Papalia, R.L. Rich, B.K. Gale, D.G. Myszka, Anal. Biochem. 373 (2008) 141.
[10] C. Hultschig, J. Kreutzberger, H. Seitz, Z. Konthur, K. Bussow, H. Lehrach, Curr. Opin. Chem. Biol. 10 (2006) 4.
[11] C.A. Rowe, S.B. Scruggs, M.J. Feldstein, J.P. Golden, F.S. Ligler, Anal. Chem. 71 (1999) 433.
[12] M. Wolf, M. Zimmermann, E. Delamarche, P. Hunziker, Biomed. Microdevices 9 (2007) 135.
[13] M. Zimmermann, E. Delamarche, M. Wolf, P. Hunziker, Biomed. Microdevices 7 (2005) 99.
[14] M. Wolf, D. Juncker, B. Michel, P. Hunziker, E. Delamarche, Biosens. Bioelectron. 19 (2004) 1193.
[15] S. Cesaro-Tadic, G. Dernick, D. Juncker, G. Buurman, H. Kropshofer, B. Michel, C. Fattinger, E. Delamarche, Lab. Chip. 4 (2004) 563.
[16] A. Bernard, B. Michel, E. Delamarche, Anal. Chem. 73 (2001) 8.
[17] A. Bernard, D. Fitzli, P. Sonderegger, E. Delamarche, B. Michel, H.R. Bosshard, H. Biebuyck, Nat. Biotechnol. (2001) 866.
[18] E. Delamarche, A. Bernard, H. Schmid, B. Michel, H. Biebuyck, Science 276 (1997) 779.
[19] B.M. Murphy, X.Y. He, D. Dandy, C.S. Henry, Anal. Chem. 80 (2008) 444.
[20] M. Wolin, H.K. Mohazzab, in: J.G. Scandalios (Ed.), Oxidative Stress and the Molecular Biology of Antioxidant Defenses, Cold Spring Harbor Laboratory Press, Plainview, NY, 1997, p. 21.
[21] S.J. Klebanoff, Ann. Intern. Med. 93 (1980) 480.
[22] Y.J. Zhang, Y.F. Xu, X.Q. Chen, X.C. Wang, J.Z. Wang, FEBS. Lett. 579 (2005) 2421.
[23] M. Dizdaroglu, P. Jaruga, M. Birincioglu, H. Rodriguez, Free Rad. Biol. Med. 32 (2002) 1102.
[24] M. Inouye, T. Mio, K. Sumino, Atherosclerosis 148 (2000) 197.
[25] P.J. Chowienczyk, S.E. Brett, N.K. Gopaul, D. Meeking, M. Marchetti, D.L. Russell-Jones, E.E. Anggard, J.M. Ritter, Diabetologia 43 (2000) 974.
[26] H. Esterbauer, R. Schmidt, M. Hayn, in: H. Sies (Ed.), Advances in Pharmacology, Academic Press, San Diego, 1997, p. 425.
[27] T. Finkel, N.J. Holbrook, Nature 408 (2000) 239.
[28] H. Sies (Ed.), Oxidative Stress, Academic Press, London, 1985.
[29] P.K. Smith, R.I. Krohn, G.T. Hermanson, A.K. Mallia, F.H. Gartner, M.D. Provenzano, E.K. Fujimoto, N.M. Goeke, B.J. Olson, D.C. Klenk, Anal. Biochem. 150 (1985) 76.
[30] L.G. Wood, P.G. Gibson, M.L. Garg, J. Sci. Food Agric. 86 (2006) 2057.
[31] R. Mateos, L. Bravo, J Sep. Sci. 30 (2007) 175.
[32] B. Halliwell, M. Whiteman, Brit. J. Pharmacol. 142 (2004) 231.
[33] T. England, E. Beatty, A. Rehman, J. Nourooz-Zadeh, P. Pereira, J. O'Reilly, H. Wiseman, C. Geissler, B. Halliwell, Free Rad. Res. 32 (2000) 355.
[34] D. Juncker, B. Michel, P. Hunziker, E. Delamarche, Biosens. Bioelectron. 19 (2004) 1193.
[35] B. Trotter, G. Moddel, R. Ostroff, G.R. Bogart, Opt. Eng. 38 (1999) 902.
[36] P. Englebienne, Immune and Receptor Assays in Theory and Practice, CRC Press, Boca Raton, 2000.

[37] J.C. McDonald, D.C. Duffy, J.R. Anderson, D.T. Chiu, H.K. Wu, O.J.A. Schueller, G.M. Whitesides, Electrophoresis 21 (2000) 27.
[38] J.A. Vickers, C.S. Henry, Electrophoresis 26 (2005) 4641.
[39] E. Diamandis, T.K. Christopoulos, Immunoassay, Academic Press, San Diego, 1996, p. 44.
[40] J. Ziegler, M. Zimmermann, P. Hunziker, E. Delamarche, Anal. Chem. 80 (2008) 1763.
[41] E. Diamandis, T.K. Christopoulos, Immunoassay, Academic Press, San Diego, 1996, p. 47.
[42] D. Rodbard, Anal. Biochem. 90 (1978) 1.